Segmental Relaxation in Macromolecules

ANGELO PERICO

Centro di Studi Chimico-Fisici di Macromolecole Sintetiche e Naturali, CNR and Istituto di Chimica Industriale, Università di Genova, Corso Europa 30, 16132 Genova, Italy

Received January 3, 1989 (Revised Manuscript Received June 6, 1989)

Much of the richness of the properties displayed by polymers in technology and biology is due to the flexibility of the long polymer chain. In the liquid state, a polymer not only translates but continuously changes its configuration due to thermal motion. If the time scale is long enough to average out the fast inertial motions ($t \gg$ picoseconds),[1] these intramolecular dynamics can be described as a diffusive motion between different configurations or states in a complicated intramolecular potential. The long relaxation times correspond to the regime of long-wavelength modes of motion, which are strongly molecular weight dependent. These modes are dominated by excluded volume and hydrodynamic interaction effects in dilute solutions, and by the screened excluded volume and hydrodynamic interactions in semidilute nonentangled solutions.[2] For these long-wavelength modes, the conformational details of the chain can be ignored and a simple universal model can be introduced. As the time scale decreases, the spatial range of the motion decreases and, on the nanosecond time scale, segmental motions are observed. These motions are almost independent of molecular weight but are strongly dependent on the local conformational details of the polymer, and they retain some dependence on the excluded volume and hydrodynamic interactions.[3]

If the polymer is a collection of different units, the conformational energy function of each unit must be specified together with the correlations with the neighboring units. As a result, a biological macromolecule built of different units, such as the amino acids of a protein, displays different static and dynamic local properties. The differences are found not only at the chain ends but also at each unit, according to its specific structure and its neighboring interactions. On the contrary, a homopolymer displays different statistical and dynamic local properties only for a relatively small number of units at the chain ends. This is the reason why biological macromolecules display such different local domains of different flexibility and mobility, strongly related to biological functions.[4,5]

Segmental motions in the nanosecond time range are probed by dynamic scattering, NMR and dielectric relaxation, ESR, intramolecular excimer formation, and fluorescence anisotropy. Of particular importance are the measurements probing the orientational time autocorrelation functions of one segment vector belonging to the chain. This is the case of the fluorescence anisotropy decay of a chromophore naturally present on, or rigidly attached as a label to, the chain. Time-resolved fluorescence using mode-locked picosecond pulsed lasers, picosecond holographic grating techniques, and frequency domain fluorometry are alternatively used.[6-8] Several synthetic polymers, such as polystyrene and polyisoprene, have been labeled in the main chain with anthracene to study segmental dynamics by fluorescence anisotropy.[9,10] The advantage of this main-chain labeling with anthracene is that the transition dipole moment (the relaxing segment) lies along the backbone. Examples of naturally labeled polymers include polypeptides and proteins containing a single fluorescent group, normally a tryptophan or a tyrosine (as in the ACTH hormone or in azurin).[6,8]

The frequency dependence of NMR, and especially of ^{13}C NMR relaxation times T_1 and T_2 and nuclear Overhauser effect, also produces useful information.[3] The advantage of this technique is that it does not require the introduction of any type of labeling, and therefore it applies to any polymer. However, the spectral density is normally tested only at few frequencies. A large body of experimental results has been published resulting from both the fluorescence anisotropy[7,9-15] and the ^{13}C NMR[16-25] techniques. Other dy-

Angelo Perico was born in Quiliano (Savona), Italy, in 1941. He received a doctoral degree in Physics from the University of Genova in 1964. He joined the Institute of Industrial Chemistry, University of Genova, first as Research Assistant in Theoretical Chemistry and then as a researcher of the Italian National Research Council (CNR). Since 1975 he has been at the Centro di Studi Chimico-Fisici di Macromolecole Sintetiche e Naturali of the CNR, University of Genova, where he was appointed Director in 1987. His research is currently focused on hydrodynamics, dynamics, and intramolecular reactions of polymers.

(1) Chandrasekhar, S. *Rev. Mod. Phys.* **1943**, *15*, 1-89.
(2) Doi, M.; Edwards, F. S. *The Theory of Polymer Dynamics*; Clarendon Press: Oxford, 1986.
(3) Bailey, R. T.; North, A. M.; Pethrik, R. A. *Molecular Motion in High Polymers*; Clarendom Press: Oxford, 1981.
(4) Clementi, E., Chin, S., Eds. *Structure and Dynamics of Nucleic Acids, Proteins and Membranes*; Plenum Press: New York, 1986.
(5) Karplus, M.; McCammon, J. A. *Annu. Rev. Biochem.* **1983**, *53*, 263-300.
(6) Chen, L. X. Q.; Petrich, J. W.; Fleming, G. R.; Perico, A. *Chem. Phys. Lett.* **1987**, *139*, 55-61.
(7) Hyde, P. D.; Waldow, D. A.; Ediger, M. D.; Kitano, T.; Ito, K. *Macromolecules* **1986**, *19*, 2533-2538.
(8) Alcala, J. R.; Gratton, E.; Prendergast, F. G. *Biophys. J.* **1987**, *51*, 587-596; 597-604; 925-936.
(9) Valeur, B.; Monnerie, L. *J. Polym. Sci., Polym. Phys. Ed.* **1976**, *14*, 11-27.
(10) Monnerie, L.; Viovy, J. L. In *Photophysical and Photochemical Tools in Polymer Science*; Winnik, M. A., Ed., Nato ASI C182: Dordrecht, 1986; pp 193-224 and references therein.
(11) Viovy, J. L.; Monnerie, L.; Brochon, J. L. *Macromolecules* **1983**, *16*, 1845-1852.
(12) Viovy, J. L.; Monnerie, L.; Merola, F. *Macromolecules* **1985**, *18*, 1130-1137.
(13) Waldow, D. A.; Johnson, B. S.; Babiarz, C. L.; Ediger, M. D.; Kitano, T.; Ito, K. *Polym. Commun.*, to be published.
(14) Waldow, D. A.; Johnson, B. S.; Hyde, P. D.; Ediger, M. D.; Kitano, T.; Ito, K. *Macromolecules*, to be published.
(15) Hyde, P. D.; Ediger, M. D.; Kitano, T.; Ito, K. *Macromolecules*, to be published.
(16) Laupretre, F.; Noel, C.; Monnerie, L. *J. Polym. Sci., Polym. Phys. Ed.* **1977**, *15*, 2127-2142; 2143-2149.
(17) Laupretre, F.; Monnerie, L.; Vogl, O. *Eur. Polym. J.* **1978**, *14*, 981-984.
(18) Tekely, P.; Laupretre, F.; Monnerie, L. *Macromolecules* **1983**, *16*, 415-420.
(19) Jones, A. A.; Stockmayer, W. H. *J. Polym. Sci., Polym. Phys. Ed.* **1977**, *15*, 847-861.

0001-4842/89/0122-0336$01.50/0

namic techniques have been proposed or may be devised to solve specific problems.[26]

In any case, the crucial point for a quantitative interpretation of these relaxation experiments (and of the correlate technological properties or site-specific biological functions) is the availability of reliable models relating the measured time correlation functions (TCFs) to the local structural complexity of the chain. There are still enormous difficulties in obtaining theoretically well founded procedures, although some relevant progress has been achieved recently. Here we review these advancements and discuss the resulting measurable TCFs. Theoretical models for the orientational TCFs governed by diffusion were solved early for rods, spheres, and ellipsoids by Debye[27] and Perrin.[28] Only in 1985 was an exact solution to these TCFs given[29,30] for flexible and semiflexible polymers, in the framework of an optimum approximation to the generalized diffusion equation in the full configuration space.[31,32] Note that even the simple case of the TCFs of a Gaussian bead spring model was unsolved and rough approximations were adopted.[31] When projection operator techniques and the memory function formalism[33] are used, an optimum solvable approximation, the optimized Rouse–Zimm (ORZ) approximation,[34,35] can be derived from the generalized diffusion equation for non-Gaussian chains. The ORZ theory strongly improves[36-38] the bare Rouse–Zimm Gaussian approximation since it includes many of the conformational details required for the description of dynamic properties in the range of nanoseconds.[29]

All the TCFs of interest in segmental relaxation experiments have been exactly derived in the ORZ dynamic approximation by Perico and Guenza.[29] The resulting ORZ local dynamics (ORZLD) are given as a sensitive function of the details of the intramolecular potential and of the specific position along the chain of the relaxing segment, and they are easily amenable to calculations. However, strong theoretical improvements are still required, especially for checking the approximations in the dynamic equations. Meanwhile, it is worth subjecting these recent theoretical advances in the calculations of the TCFs to critical comparison with experiments, as they represent a substantial improvement of the previously used[39,40] TCFs. The large body of data on local dynamics produced both in synthetic and biological macromolecular solutions could be better analyzed and correlated with real parameters giving indications for further theoretical progress.

The diffusion equation with constraints proposed by Fixman[41,42] is an improvement of the generalized Gaussian formalism of Bixon and Zwanzig (ORZ) devised to take into account constraints on bond lengths and valence angles. Relevant corrections in the mode TCFs relative to local motions are obtained for simple worm models and expected for real chains. The ORZLD approach to the calculation of the local TCFs could be extended to include some of these improvements, by changing the definition of the diffusion matrix using Fixman's constraint matrices.

Other approaches to segmental dynamics[39,40] based on Kramers theory are limited to the dynamics of the central segment of a perfectly flexible chain in free draining conditions and to the calculation of the nonobservable conformational TCF. This TCF, with the form of an exponential times a zero order modified Bessel function,[39] has been largely used in the interpretation of segmental relaxation data.[10] The assumption was made that it is representative of all the measured TCFs and that conformational details affect only the time constants of the function. Recently,[38] we have shown that the ORZLD theory gives an equivalent function for the ideal chain in the same conditions reported above. This equivalence is really not surprising when we think that the diffusion Smoluchowski equation must be equivalent to Kramers rate theory in the overdamped regime, if the same intramolecular potential is used.[43] However, ORZLD theory gives strongly different functions for different observable TCFs and different local details.

Note that one of the main differences between the orientational TCFs of a Gaussian chain and the TCFs of a "real" chain in the ORZLD approximation lies in the fact that the latter approach can take into account accurate details of the intramolecular potential including some influence of the height of the barriers. Dynamic properties of semiflexible chains[29,30] and of models in the rotational isomeric state approximation with independent or interdependent rotations (the RIS–ORZ hierarchy) have been obtained.[37,38] Recently an extension to biological macromolecules was given, including polypeptides of known intramolecular energy map of each residue, and multiple domain chains.[48]

Alternatively, molecular dynamic simulations developed in the picosecond region[5] can be extended to-

(20) Heatley, F.; Begun, A. *Polymer* **1976**, *17*, 399–408; **1977**, *18*, 637–637.
(21) Heatley, F.; Cox, M. *Polymer* **1977**, *18*, 225–232.
(22) Jones, A. A.; Robinson, G. L.; Gerr, F. E.; Bisceglia, M.; Shostak, S. L.; Lubianez, R. P. *Macromolecules* **1980**, *13*, 95–99.
(23) Heatley, F. *Prog. Nucl. Magn. Reson. Spectrosc.* **1979**, *13*, 47–85.
(24) Hung, C.-C.; Shibata, J. W.; Tarpey, M. F.; Jones, A. A.; Porco, J. A.; Inglefield, P. T. *Macromolecules*, to be published.
(25) Hung, C.-C.; Shibata, J. W.; Jones, A. A.; Inglefield, P. T. *Macromolecules*, to be published.
(26) Huber, R.; Bennet, W. S., Jr. *Biopolymers* **1983**, *22*, 261–279.
(27) Debye, P. *Polar Molecules*; Dover: New York, 1929.
(28) Perrin, F. *J. Phys. Radium* **1934**, *V*, 497; **1936**, *VII*, 1.
(29) Perico, A.; Guenza, M. *J. Chem. Phys.* **1985**, *83*, 3103–3109.
(30) Perico, A.; Guenza, M. *J. Chem. Phys.* **1986**, *84*, 510–516.
(31) Kirkwood, J. G. *Recl. Trav. Chim. Pays-Bas* **1949**, *68*, 648–657.
(32) Wax, N., Ed. *Selected Papers on Noise and Stocastic Processes*; Dover: New York, 1954.
(33) Zwanzig, R. In *Lectures in Theoretical Physics III*; Brittin, E., Downs, B. W., Downs, J., Eds.; Interscience: New York, 1961; pp 106–141.
(34) Zwanzig, R. *J. Chem. Phys.* **1974**, *60*, 2717–2720.
(35) Bixon, M.; Zwanzig, R. *J. Chem. Phys.* **1978**, *68*, 1896–1902.
(36) Perico, A.; Bisio, S.; Cuniberti, C. *Macromolecules* **1984**, *17*, 2686–2689.
(37) Perico, A.; Ganazzoli, F.; Allegra, G. *J. Chem. Phys.* **1987**, *87*, 3677–3686.
(38) Perico, A. *J. Chem. Phys.* **1988**, *88*, 3996–4000.
(39) Hall, C. K.; Helfand, E. *J. Chem. Phys.* **1982**, *77*, 3275–3282.
(40) Helfand, E. In *Photophysical and Photochemical Tools in Polymer Science*; Winnik, M. A., Ed.; Nato ASI C182: Dordrecht, 1986; pp 152–191.
(41) Fixman, M. *J. Chem. Phys.* **1988**, *89*, 2442–2462.
(42) Fixman, M.; Kovacs, J. *J. Chem. Phys.* **1974**, *61*, 4939–4949; 4950–4954.
(43) Moro, G.; Ferrarini, A.; Polimeno, A.; Nordio, P. L. In *Reactive and Flexible Molecules in Liquids*; Dorfmuller, Th., Ed.; Kluwer Academic Publishers: Dordrecht, 1989.
(44) Perico, A. *Biopolymers*, to be published.
(45) Perico, A.; Piaggio, P.; Cuniberti, C. *J. Chem. Phys.* **1975**, *62*, 4911–4918.
(46) Freed, K. F. *Macromolecules* **1983**, *16*, 1855–1862.
(47) Douglas, J. F.; Freed, K. F. *Macromolecules* **1985**, *18*, 2445–2454.
(48) Freed, K. F. *Renormalization Group Theory of Macromolecules*; John Wiley and Sons: New York, 1987.

ward the nanosecond domain. However, this requires computing times of the order of many hours in a modern supercomputer, and even the simplified Brownian dynamics techniques are still quite time consuming. In addition, an understanding of the main parameters of the underlying processes is better achieved by retaining the typical reductionist approach of the physical sciences through a modelization.

The ORZ Local Dynamics

The linear macromolecular chain is modeled as a collection of n beads (monomer or effective monomer units) of coordinates $\mathbf{R}_i$ and frictional coefficients ζ_i, connected by a potential of mean force $V(\{\mathbf{R}_i\})$ and fluctuating due to Brownian motion. The bonds connecting neighboring beads are assumed to have root mean square length l_i. For the sake of simplicity, we assume here that all the ζ_i and l_i are identical with ζ and l. The intramolecular potential $V(\{\mathbf{R}_i\})$ can take into account the structural properties of each unit in the chain together with their short-range correlations, including the form of the potential and the heights of the barriers. Excluded volume interactions can be included by using suitable approximations[45-47] supported by exact renormalization group calculations,[48] but here these are discarded in favor of simpler θ conditions.

With each bond vector $\mathbf{l}_i$

$$\mathbf{l}_i = \mathbf{R}_i - \mathbf{R}_{i-1} \qquad i = 1, ..., n-1 \tag{1}$$

in position i along the chain, we associate the TCFs of experimental interest related to the first and second Legendre polynomials:

$$P_1^i(t) = \langle \cos \theta^i(t) \rangle = \langle [\mathbf{l}_i(t)\cdot\mathbf{l}_i(0)]/l_i(t)l_i(0) \rangle \tag{2}$$

$$P_2^i(t) = \langle \tfrac{3}{2} \cos^2 \theta^i(t) - \tfrac{1}{2} \rangle = \tfrac{3}{2}\langle [\mathbf{l}_i(t)\cdot\mathbf{l}_i(0)]^2/l_i^2(t)l_i^2(0) \rangle - \tfrac{1}{2} \tag{3}$$

with $\theta^i(t)$ the angle the bond vector $\mathbf{l}_i$ rotates in time t.

These TCFs are related to dielectric relaxation, fluorescence anisotropy, and NMR relaxation times by

$$\frac{\epsilon - \epsilon_\infty}{\epsilon_0 + \epsilon_\infty} = -\int_0^\infty \frac{dP_1(t)}{dt} \exp(-i\omega t)\, dt \tag{4}$$

$$r^i(t)/r_0^i = P_2^i(t) \tag{5}$$

$$J^i(\omega) = \mathrm{Re} \int_0^\infty P_2^i(t) \exp(-i\omega t)\, dt \tag{6}$$

with ϵ the dielectric constant, $r^i(t)$ the fluorescence anisotropy, and $J^i(\omega)$ the NMR spectral density. In addition, we define the fundamental TCF of the vector $\mathbf{l}_i$:

$$M_1^i(t) = \langle \mathbf{l}_i(t)\cdot\mathbf{l}_i(0) \rangle / \langle l_i^2 \rangle \tag{7}$$

The dynamic equation required to calculate these TCFs was chosen[29] to be the ORZ approximation to the generalized diffusion equation in the full configuration space of the polymer. This approximation amounts to the Langevin equation[29,30,38]

$$\frac{\partial}{\partial t}\mathbf{R}_i(t) + \sigma \sum_{j=0}^{n-1} (\mathbf{HA})_{ij}\mathbf{R}_j(t) = \mathbf{v}^*_i(t) \tag{8}$$

describing the time evolution of the bead coordinates under random forces, responsible for the Gaussian random velocity $\mathbf{v}^*_i(t)$, the intramolecular potential $V(\{\mathbf{R}_i\})$, friction forces, and hydrodynamic interactions (describing interaction between friction forces and flow). The matrix $\mathbf{A}$ of order n is given in terms of the inverse $\mathbf{U}$ of the static bond correlation matrix

$$U_{ij}^{-1} = \langle \mathbf{l}_i\cdot\mathbf{l}_j \rangle / l^2 \tag{9}$$

as

$$\mathbf{A} = \mathbf{M}^{\mathrm{T}} \begin{pmatrix} 0 & 0 \\ 0 & \mathbf{U} \end{pmatrix} \mathbf{M} \tag{10}$$

with the matrix $\mathbf{M}$ of order n given as

$$\mathbf{M} = \begin{pmatrix} 1/n & 1/n & . & . \\ -1 & 1 & 0 & . \\ 0 & -1 & 1 & 0 \\ . & . & . & . \end{pmatrix} \tag{11}$$

The matrix $\mathbf{H}$ is the hydrodynamic interaction matrix averaged over the polymer configurations

$$H_{ij} = \delta_{ij} + \zeta_r \langle l/R_{ij} \rangle (l - \delta_{ij}) \tag{12}$$

with

$$\zeta_r = \zeta/6\pi\eta_0 l \tag{13}$$

the hydrodynamic interaction strength, with η_0 the solvent viscosity. In a θ solution, ζ_r has been estimated theoretically and experimentally to have the value 0.25.[45,49] The constant

$$\sigma = 3k_B T/l^2\zeta \tag{14}$$

is the typical bond rate constant of the model. A rough estimate of σ is given using eq 13, with the value 0.25, to obtain

$$\sigma \approx 2k_B T/\pi\eta_0 l^3 \tag{15}$$

This value is expected to be an upper bound to the jump rate of a bond, while in a quantitative comparison with experiments, σ should be allowed to change as a smooth parameter in order to compensate for the approximations in the ORZ approach. The bond vector static correlation matrix and mean inverse distances $\langle l/R_{ij} \rangle$ are better computed exactly by using the full intramolecular potential $V(\{\mathbf{R}_i\})$:

$$\langle l_i\cdot l_j \rangle / l^2 = N \int d\{\mathbf{R}_i\} \exp[-V(\{\mathbf{R}_i\})/k_B T](\mathbf{l}_i\cdot\mathbf{l}_j)/l^2 \tag{16}$$

$$\langle l/R_{ij} \rangle = N \int d\{\mathbf{R}_i\} \exp[-V(\{\mathbf{R}_i\})/k_B T](l/R_{ij}) \tag{17}$$

with

$$N^{-1} = \int d\{\mathbf{R}_i\} \exp[-V(\{\mathbf{R}_i\})/k_B T] \tag{18}$$

or via the Gaussian approximation

$$\langle l/R_{ij} \rangle = (6/\pi)^{0.5} \langle R_{ij}^2 \rangle^{-0.5} \tag{19}$$

$$\langle R_{ij}^2 \rangle = l^2 \sum_{p,q=i+1}^{j} U_{pq}^{-1} \qquad j > i \tag{20}$$

In approximation 19, all the conformational information enters into the ORZ dynamics via $\mathbf{U}^{-1}$. We note from eq 16 that the ORZ dynamics include some information on the form and barrier heights if we choose a detailed intramolecular energy map. It is worth re-

(49) Osaki, K.; Schrag, J.; Ferry, J. *Macromolecules* **1972**, *5*, 144-147.

calling that in the ORZ approximation some information on the conformational energy (affecting moments higher than the second) and some contributions to the diffusion tensor are lost with the discarded memory or by ignoring local constraints. Both these effects may have appreciable influence on the local dynamic scale. Much more theoretical work in this direction is required.

In spite of the ignored contributions, the ORZ approximation strongly improves the Rouse–Zimm Gaussian approximation. This allows for a first account not only of long-wavelength relaxation modes on a spatial scale greater than a Kuhn effective segment but also of short-wavelength modes, characterizing cooperative local motions on a scale greater than the bond length in the nanosecond time domain. The validity of this account will be checked by experiments and by improvement of the basic theoretical approach.

In θ solutions, the concentration effects to first order may be included by using the discrete full dynamic multiple scattering approach (DDMS theory), which maintains its validity for all the hierarchy of dynamic ORZ models.[50] Higher order effects can be approximately included by introducing the concept of screening of the hydrodynamic interaction, while concentrated solutions in good solvents require major efforts to include the tube model description.[2]

A local persistence length relative to the bond i as the mean projection of the bond vector i on the end-to-end vector distance of the chain was introduced as follows:[44]

$$P_n^i/l = \sum_{j=1}^{n-1}\langle \mathbf{l}_i\cdot\mathbf{l}_j\rangle/l^2 = \sum_{j=1}^{n-1} U_{ij}^{-1} \qquad (21)$$

This length describes the number of bonds statistically aligned with bond i. This definition takes into account interactions both with preceding and following bonds because the bond position may be strongly asymmetric. The persistence length P_n^i is sensitive to the chemical composition of the chain and, for a short or very stiff finite chain, to the length of the chain. With definition 21, the characteristic ratio for the finite chain C_n turns out to be the average of the bond persistence lengths:

$$\bar{P}_n/l = (n-1)^{-1}\sum_{i=1}^{n-1} P_n^i \equiv C_n \qquad (22)$$

Solving eq 8 by transformation to normal coordinates $\{\xi_a\}$, we get[29] for the fundamental TCF $M_1^i(t)$:

$$M_1^i(\tau) = \sum_{a=1}^{n-1}(Q_{ia} - Q_{i-1,a})^2\mu_a^{-1}\exp(-\lambda_a\tau) \qquad (23)$$

with

$$\tau = \sigma t \qquad (24)$$

the normalized time in σ^{-1} units. The quantities $\mathbf{Q}$ and $\{\lambda_a\}$ are the matrix of eigenvectors and the eigenvalues of the product matrix $\mathbf{HA}$, while μ_a^{-1} is proportional to the mean square length of the normal mode ξ_a:

$$\langle \xi_a^2\rangle = l^2\mu_a^{-1} \qquad (25)$$

Note that $\mathbf{Q}$, $\{\lambda_a\}$, and $\{\mu_a\}$ characterize each model of the ORZ hierarchy, and in the simple Gaussian approximation for the $\langle l/R_{ij}\rangle$, eq 17, these parameters are only a function of the static bond correlation matrix $\mathbf{U}^{-1}$.

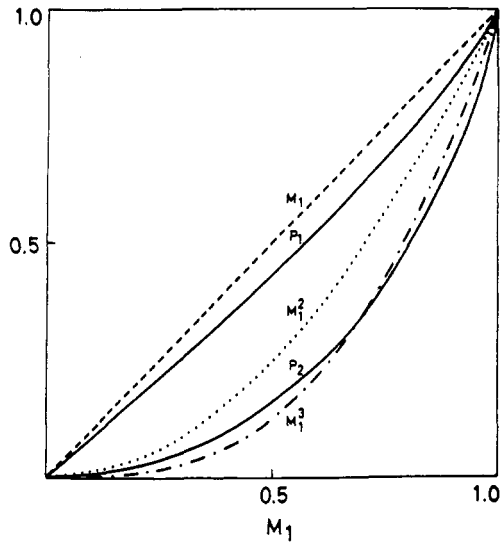

Figure 1. The first- and second-order TCFs, $P_1(t)$ and $P_2(t)$ (—) and the segment vector autocorrelation function M_1 (– –) together with M_1^2 (···) and M_1^3 (–·–) versus M_1. From ref 29.

For the first- and second-order TCFs, the following results were obtained exactly[29] in the ORZ approximation (eq 8) to the generalized diffusion equation:

$$P_1^i(t) = (1-x^2)[1 - (2/\pi)\arctan x] + (2/\pi)x \qquad (26)$$

$$P_2^i(t) = 1 - 3\{x^2 - x^3(\pi/2)[1 - (2/\pi)\arctan x]\} \qquad (27)$$

where

$$x = [1 - (M_1^i(t))^2]^{0.5}/M_1^i(t) \qquad (28)$$

Equations 25–27 show that in the ORZ approximation $P_1^i(t)$ and $P_2^i(t)$ are universal functions of the i bond vector TCF, $M_1^i(t)$.

The static bond correlation matrix $\mathbf{U}^{-1}$ has a central role in the ORZLD theory because all the conformational details enter into the theory via this matrix. Note that if the segmental relaxation is described by P_1^i or P_2^i, the effects of the position of the bond along the chain and of the polymer structure enter only via M_1^i, eq 23, through λ_a, μ_a, and $(Q_{ia} - Q_{i-1,a})^2$.

Main Results of the ORZLD Theory

In Figure 1 the universal plot of $P_1^i(t)$ and $P_2^i(t)$ against $M_1^i(t)$ is presented.[29] The plot is valid for any ORZ model and for any bond i in the chain. In the same plot, $M_1^i(t)$, $(M_1^i(t))^2$, and $(M_1^i(t))^3$ are shown. The figure clearly shows that the first-order TCF P_1 is different from the bond vector TCF M_1 over the entire time range. The TCF P_2 is shown to be strongly different from M_1^2 and rather different from M_1^3, the characteristic second-order TCF for a sphere or a rod. We note that this general conclusion is in striking contradiction with the simple assumptions, often reported in literature, according to which P_1 is approximated by M_1 and P_2 by M_1^2 and with the models based on tetrahedral lattices, according to which $P_1 = P_2$.

In the simplest model in the ORZ hierarchy, the Gaussian bead spring model, we analytically know the quantities $\mathbf{Q}$, $\{\lambda_a\}$, and $\{\mu_a\}$ exactly in the free draining Rouse limit and within an accurate approximation in the nondraining Zimm limit. These analytical quan-

(50) Perico, A.; La Ferla, R.; Freed, K. F. *J. Chem. Phys.* **1987**, *86*, 5842–5851.

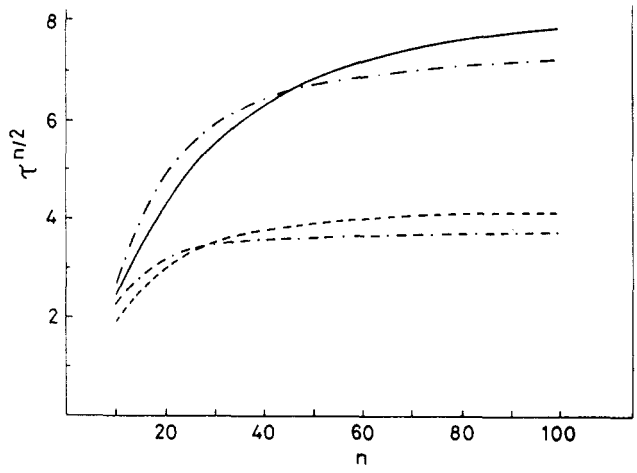

Figure 2. The correlation time $\tau^{n/2}$ for the TCF $P_2^{n/2}(t)$: iPS (—), PE (-·-), iPP (--), and PDMS (-··-). From ref 38.

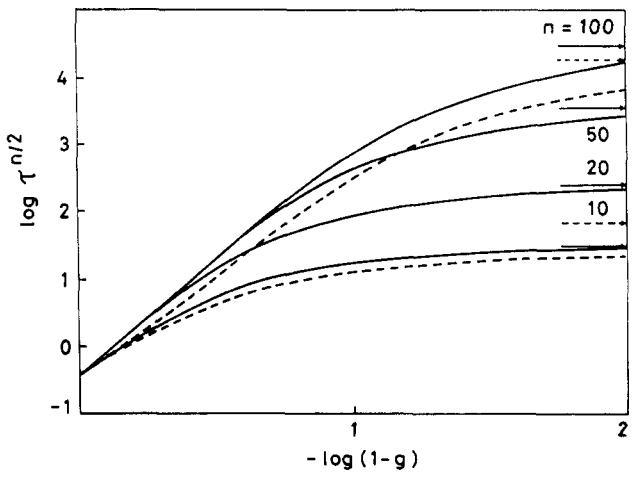

Figure 3. The correlation time $\tau^{n/2}$ for the TCF $P_2^{n/2}(t)$ vs the numerical persistence length $P/l = (1 - g)^{-1}$ for n = 10, 20, 50, 100: rod limits (arrows); $\zeta_r = 0$ (—); $\zeta_r = 0.25$ (--). From ref 30.

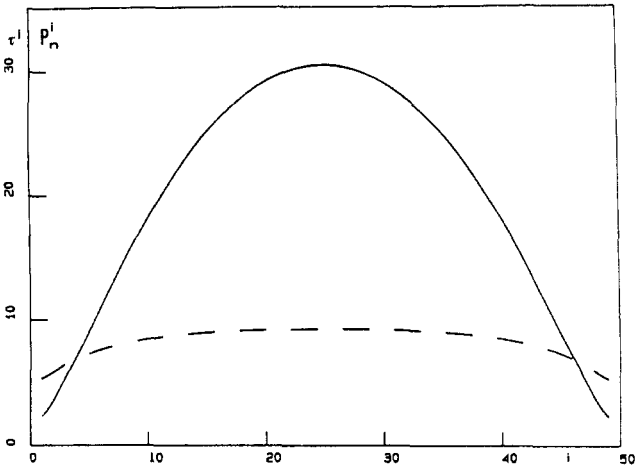

Figure 4. The bond correlation times τ^i (for $P_2^i(t)$) (—) and local persistence lengths P_n^i/l (--) as a function of the bond index i for poly-L-alanine, n = 50. From: Perico, A. *Biopolymers*, to be published.

tities allowed us to obtain exact expressions of M_1 for the central and end bonds:[38]

$$M_1^{n/2}(\tau) = \exp(-2\tau)I_0(2\tau) \quad (29)$$

$$M_1^{1}(\tau) = \exp(-2\tau)I_1(2\tau)/\tau \quad (30)$$

in the free draining case and

$$M_1^{n/2}(\tau) \simeq (2/3)(\alpha\tau)^{-2/3}[\gamma(2/3,\alpha\tau) - \gamma(2/3,\alpha\tau/n^{2/3})] \quad (31)$$

$$M_1^{1}(\tau) \simeq (2/3)\sum_{k=1}^{\infty}\frac{(-1)^{k+1}(2\pi)^{2k}}{(2k)!(\alpha\tau)(4k+2)/3}\left[\gamma\left(\frac{4k+2}{3},\alpha\tau\right) - \gamma\left(\frac{4k+2}{3},\alpha\tau/n^{3/2}\right)\right] \quad (32)$$

in the nondraining case. Here $I_m(x)$ is the modified Bessel function of order m, and $\gamma(a,x)$ the incomplete γ function. Note that eq 31 and 32 simplify to the first term for large n and τ not too large. A comparison of eq 29 and 32 shows quite clearly the difference in the relaxing behavior of bonds in a central or an end position as well as a strong draining effect. The latter effect is indicative of a concentration dependence because, in passing from diluted to concentrated, nonentangled solutions, the hydrodynamic interactions become screened. Theory predicts by simple small τ and asymptotic expansions of eq 29 and 32 that in the short-time behavior there are no draining and position effects, while these effects become strong in the long-time behavior.[38] It is interesting to note that eq 29 is coincident[38] with the main result derived by Helfand and co-workers[30,40] for a conformational transition model in a Kramers-type approach, if their conformational TCF, $C(\tau)$, is identified with the present bond vector TCF, M_1. Helfand's zero order modified Bessel function behavior describes simply the connectivity for a relaxing central segment in a Gaussian chain in the free draining limit. Therefore, the success of this function in the interpretation of a large body of experimental results obtained by fluorescence anisotropy and NMR appears to be not at all unjustified. However, it also clearly appears that each specific experiment must be interpreted with the right TCF, P_1 or P_2, and that each sample requires the introduction of its proper conformational details, included in $V(\{\mathbf{R}_i\})$, avoiding the oversimplifications of the simple Gaussian chain model. In the latter case, the relaxation depends only on one parameter included in σ, say the effective bond length l. However, in the real case, the relaxation depends on all the parameters characterizing the intramolecular potential $V(\{\mathbf{R}_i\})$ (see eq 16) that include the specific rotational potential due to each unit (including the barrier height!) and its neighboring correlations. Some ORZLD results are discussed in the following for different polymer models: RIS models (including interdependence of dihedral rotations but ignoring barrier heights), semiflexible chains as described by a freely rotating chain in the ORZ approximation, polypeptide models calculated by using detailed energy maps for each residue and multiple domain chain models.

As a first example, we show[38] in Figure 2 the P_2 correlation times for a central segment,

$$\tau^{n/2} = \int_0^{\infty} P_2^{n/2}(\tau)\, d\tau \quad (33)$$

for rotational isomeric state models of polyethylene (PE), isotactic polystyrene (iPS), isotactic polypropylene (iPP), and poly(dimethylsiloxane) (PDMS) at 400 K.[37] While the end bond is almost independent

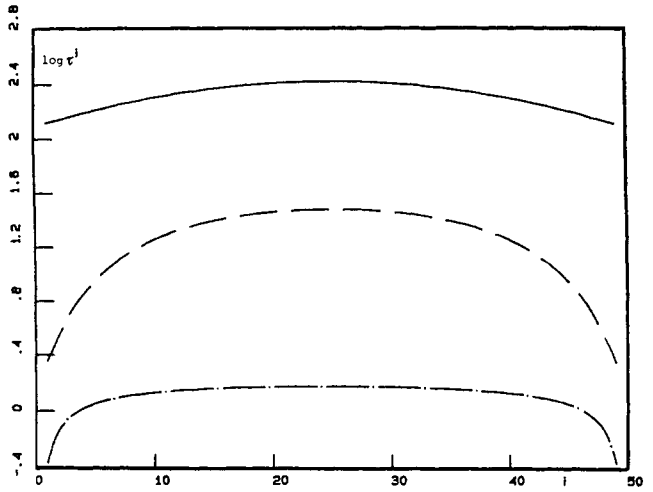

Figure 5. The bond correlation times τ^i as a function of the bond index i, $n = 50$: poly-L-prolyne II (—), poly-L-alanine (– –), and polyglycine (–·–). From: Perico, A. *Biopolymers*, to be published.

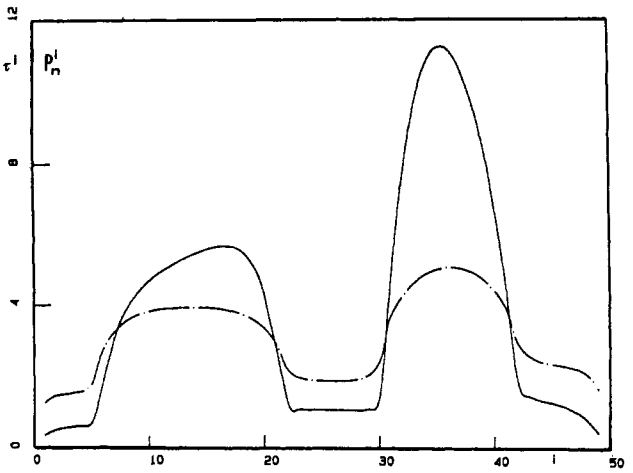

Figure 6. The bond correlation times τ^i (—) and local persistence lengths P_n^i/l (–·–) for a multiple domain chain in the ORZ freely rotating chain model; $n = 50$. From: Perico, A. *Biopolymers*, to be published.

of the number of virtual bonds for $n > 5$, the central bond displays a noteworthy increase of the correlation time $\tau^{n/2}$ with n toward an asymptotic limit almost 1 order of magnitude higher than τ^1. In addition, the larger the polymer local stiffness, the larger the observed increase: approximately 100 virtual bonds for iPS, but only 30 virtual bonds for the more flexible PDMS, are required to get molecular weight independent correlation times. This shows how large the cooperativity and sensitivity to local conformational details are in the ORZLD approach, even for flexible polymers.

For a semiflexible polymer model[30] we choose the freely rotating chain in the ORZ approximation with stiffness parameter $g = -\cos\theta$, with θ the valence angle, and numerical persistence length $P/l = (1-g)^{-1}$. Figure 3 shows[30] the correlation time (eq 33) for a central bond as a function of the numerical persistence length $(1-g)^{-1}$. For $g = 0$, the ORZ model for the freely rotating chain gives the Gaussian chain behavior, and the correlation time for P_2 becomes molecular weight independent. As g increases, the correlation time increases strongly to approximate in the $g \rightarrow 1$ limit the rod behavior, represented in the figures by the arrows. Note that, even in the rod limit, the ORZ local dynamics are accurate.

Using Flory's $\langle \mathbf{T} \rangle$ matrices calculated from the single amino acid energy map including interdependence of $\{\phi,\psi\}$ angles and the approximation of independent successive residues, the correlation times and local persistence lengths were calculated. The results are presented in Figures 4 and 5 for poly-L-alanine, polyglycine, and poly-L-prolyne II as a function of the position of the amino acid along the chain.[44] Local persistence length (hereafter normalized to the segment length l) and local dynamics appear strongly correlated, and the curves, typical for homopolymers, are bell shaped with a maximum value in the middle and with the absence of any particular domain of flexibility. However, if the polymer is built with different amino acid units, some domains of different local flexibility and dynamics can appear.[44] One of the simpler models for these chains is a freely rotating chain with different g values at different bonds. The plot in Figure 6 is relative[44] to a multiple domain chain model, characterized by five blocks of different g values. Note the emergence of five distinct static and dynamic domains, characterized by domain persistence lengths around 1.5, 3.9, 1.9, 5.0, and 2.3, while the mean persistence length is 3.12. The dynamic domains are strongly correlated with the stiffness domains and are even more pronounced.

Concluding Remarks

These concepts have been applied to the interpretation of the fluorescence anisotropy decay from single tryptophan-containing polypeptide hormones, ACTH and glucagon, and a series of their fragments.[6] As a first rough approach, an ORZ freely rotating chain model was used. The data were interpreted in terms of the effect of the position of the tryptophan along the chain, of the chain length, and of the mean persistence length. The comparisons give a reasonable value of the mean persistence length of the polypeptides, around 7–10 residues, and meaningful position effects. An interpretation of the polypeptide dynamics in terms of local persistence lengths and local dynamics using more accurate $V(\{\mathbf{R}_i\})$ potentials, calculated from peptide energy maps, is in progress. We anticipate that the emerging dynamics will be of the type shown in Figure 6. We hope that these studies will contribute insight into the role of local dynamics in the biological function of biomacromolecules.

The main goal of this paper is to summarize in a simple way the results of the ORZLD theory of segmental relaxation indicating their role in a first attempt to quantitative interpretation of segmental relaxation experiments on biological and synthetic macromolecules in terms of local conformational details. A simple magic universal function does not exist to interpret all the local dynamic features of all the synthetic and biological macromolecules in all conditions. Fortunately, the present level of the theory is still simple enough to be amenable to calculations to be checked by extensive dynamic experiments on polymer solutions.

Work is in progress to take into account, at the same theoretical level, the motion of lateral chains and of branched polymers: this step is useful in the interpretation of fluorescence anisotropy and NMR experiments.

In any case, care should be taken in the comparison with experiments, since the basic dynamic approach in the nanosecond time domain is still insufficient. In fact, the actual level of the theory (ORZLD) can be improved, by taking into account local constraints and the memory term that were discarded in the ORZ approximation to the generalized diffusion equation. Finally, more work is expected in order to clarify further the relationship between the present diffusion approach and Kramers rate theory approach.

The encouragement of Prof. M. A. Winnik of the University of Toronto and Prof. K. F. Freed of the University of Chicago is gratefully acknowledged.